

Dynamic Domain Discrepancy Adjustment for Active Multi-Domain Adaptation

Long Liu^{a,*}, Bo Zhou^a, Zhipeng Zhao^a, Zening Liu^a

^a*Xi'an University of Technology, Xi'an, 710048, China*

Abstract

Multi-source unsupervised domain adaptation (MUDA) aims to transfer knowledge from related source domains to an unlabeled target domain. While recent MUDA methods have shown promising results, most of them focus on aligning the overall feature distributions across source domains, which can lead to negative effects due to redundant features within each domain. Moreover, there is a significant performance gap between MUDA and supervised methods. To address these challenges, we propose a novel approach called Dynamic Domain Discrepancy Adjustment for Active Multi-Domain Adaptation (D³AAMDA). Firstly, we establish a multi-source dynamic modulation mechanism during the training process based on the degree of distribution differences between source and target domains. This mechanism controls the alignment level of features between each source domain and the target domain and effectively use the local advantageous feature information within the source domains. Additionally, we propose a Multi-source Active Boundary Sample Selection (MABS) strategy, which utilizes a guided dynamic boundary loss to design an efficient query function for selecting important samples. This strategy achieves improved generalization to the target domain with minimal sampling costs. We extensively evaluate our proposed method on commonly used domain adaptation datasets, comparing it against existing UDA and ADA methods. The experimental results unequivocally demonstrate the superiority of our approach.

Keywords: transfer learning, domain adaptation, active learning, discrepancy-based methods

1. Introduction

Deep neural networks have demonstrated exceptional performance when trained on large annotated datasets. However, obtaining the desired annotated data in the real world is expensive, and models trained on such datasets may struggle to generalize to new datasets and tasks due to domain shift. Unsupervised Domain Adaptation (UDA) techniques have been developed to mitigate the impact of domain shift on model performance when only unlabeled data is available in the target domain.

Early UDA methods primarily focused on single-source scenarios. However, in practical applications, multiple source domains relevant to the target domain are often accessible. Leveraging multiple source domains to enhance UDA performance is desirable. Nevertheless, due to different data collection conditions in each source domain, feature distribution discrepancies exist between each source domain and the target domain. Simply merging multiple source domain data and performing single-source domain adaptation may exacerbate domain shift. Therefore, the key to addressing multi-source domain adaptation lies in establishing an optimal domain adaptation learning process that considers the diverse feature distribution differences between each source domain and the target domain, as well as the approaches for domain transfer.

To address the aforementioned issues, some Multi-source Unsupervised Domain Adaptation (MUDA) methods (Zhao et al., 2018; Peng et al., 2019; Xu et al., 2018; Mansour et al., 2008) adopt a holistic approach to align multiple source domains with the target domain and employ weighted classification strategies at the decision level. However, these methods aim to map features from the source and target domains to a shared feature space, which may result in the loss of domain-specific representations and negative transfer. Another category of methods (Wang et al., 2020; Zhao et al., 2020) focuses on aligning inter-class features by aligning the classes of the source and target domains to obtain an optimal classifier for target domain samples. However, due to distribution differences, achieving complete alignment of class boundaries between each source domain and the target domain is challenging.

Although the methods above have demonstrated remarkable performance, they still lack sufficient consideration of the distribution differences among source domains. As depicted in Figure 1, the distribution of multi-source data is complex, with varying degrees of correlation between the overall distribution of source domains and the target domain, as well as local distribution correlations.

In more practical application scenarios, although acquiring complete labels for the target domain is challenging, it is possible to improve domain adaptation (DA) performance by selecting a small portion of target domain data for annotation within a given budget. Active learning (AL) techniques aim to select representative samples from a large pool of unlabeled samples for annotation and model training. This learning paradigm focuses on sample selection strategies, and the model training

*Corresponding author

Email addresses: liulong@xaut.edu.cn (Long Liu),
1220311012@stu.xaut.edu.cn (Bo Zhou),
2220320119@stu.xaut.edu.cn (Zhipeng Zhao),
znliu@stu.xaut.edu.cn (Zening Liu)

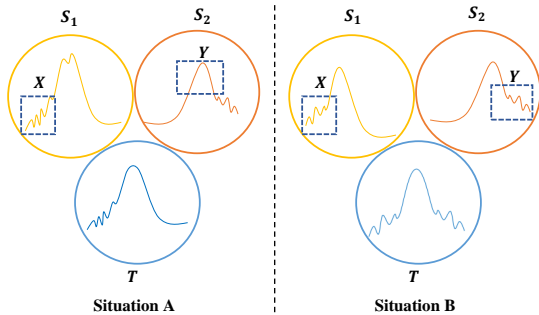


Figure 1: The local distribution relationships between source and target domains: in situation A, source domain S_1 is closer to the target domain in the overall distribution, while source domain S_1 exhibits similarity in the X segment and source domain S_2 exhibits similarity in the Y segment in terms of local distribution patterns. In situation B, both source domains S_1 and S_2 have similar differences in data distribution compared to the target domain, with source domain S_1 showing similarity in the X segment and source domain S_2 showing similarity in the Y segment.

process starts from scratch. In the context of multi-source unsupervised domain adaptation (MUDA), traditional AL methods may select anomalous or redundant instances during the selection process of target domain data due to the presence of domain shift. This contradicts our intention, as we aim to enhance MUDA performance with minimal labeling costs. Some studies (Su et al., 2020; Huang et al., 2018; Prabhu et al., 2021) have combined active learning with domain adaptation, but these methods primarily address single-source problems and are not effective in instance selection under multi-source settings.

Based on the aforementioned issues, this paper proposes the following points in the context of multi-source domain adaptation: 1) Pursuing overall alignment between multiple source domains and the target domain is not necessarily the best strategy for this problem. To preserve the target domain’s classification features as much as possible, it is essential to control the degree of feature alignment between each source domain and the target domain by weighting them based on the level of distribution differences. 2) Effective utilization of the similarity between the local distributions of different source domains and the target domain should be considered. In the process of multi-source domain adaptation, the adaptation weights for multiple domains should be dynamically adjusted based on the local distribution differences of multiple source domains to achieve an optimal learning process. 3) In the active learning sampling process, it is not sufficient to select instances based solely on the specific relationship between a single source domain and the target domain. This would result in the selection of samples biased towards a single source domain and lead to redundant sampling.

Based on the aforementioned points, this paper introduces a Dynamic Domain Discrepancy Adjustment for Active Multi-Domain Adaptation (D^3 AAMDA) method that leverages the differences between the source domain and target domain distributions. Our approach fully considers the diversity of source domain data distributions during domain adaptation by weighting the alignment of features between each source domain and the target domain based on the degree of distribution differ-

ences. We establish a dynamic objective function learning convergence mechanism. Furthermore, we propose a Multi-source Active Boundary Sample Selection (MABS) strategy. This strategy implicitly expands the boundaries between different source domain classes and amplifies the differences between similar samples across classes. Based on the dynamic domain difference modulation strategy, we select target domain samples that contain the most informative content by considering the feature relationships between difficult samples from the target domain and the source domains. These selected samples are then labeled and incorporated into the model training process. In simple terms, our active learning sample selection mechanism not only focuses on the uncertainty and diversity of the target domain data itself (Su et al., 2020; Prabhu et al., 2021) but also considers the relevance between difficult-to-classify samples from the source domains and the target domain data. At the same time, we ignore the redundancy brought by well-classified samples in the target domain sampling process.

The main contributions of our proposed method are as follows: (1) Addressing the impact of complex distribution imbalance in multi-source domain data on domain adaptation learning, we construct an adaptive learning model with a dynamic domain difference modulation strategy. We define a weighted form of the multi-source deep domain adaptation objective loss function and take into account both the overall and local distribution differences between each source domain and the target domain. We propose a dynamic domain difference modulation mechanism that dynamically adjusts the weights of each source domain in the overall loss function. (2) We introduce a Multi-source Active Boundary Sample Selection (MABS) strategy that enhances the role of difficult samples in shaping decision boundaries by employing a dynamic boundary loss. This strategy guides the model to pay more attention to the impact of difficult examples on the selection of target domain samples, by focusing on the difficulties in the classification boundaries of each source domain. Our sampling strategy aims to improve model performance with minimal annotation costs, and to the best of our knowledge, this is the first work that applies active learning to the multi-source domain adaptation problem. (3) We evaluate the performance of our method on multiple domain adaptation benchmark datasets. The experimental results demonstrate that our approach achieves state-of-the-art performance.

2. Related Work

Domain Adaptation (DA) aims to generalize models trained on the source domain to the target domain, considering the differences in their feature distributions. Early methods in DA focused on extracting domain-invariant features to achieve this goal. In recent years, some DA methods have addressed domain shift by adjusting the feature distributions between the source and target domains. For example, certain works (Tzeng et al., 2014; Sun and Saenko, 2016; Kang et al., 2019; Damodaran et al., 2018; Courty et al., 2017) minimize various metrics to align the features of the source and target domains. Other works

adopt adversarial approaches, where the training process involves a game between a feature extractor and a domain discriminator. The domain discriminator learns to differentiate between source and target domain features, while the feature extractor learns to confuse the domain discriminator by extracting domain-invariant features, ultimately aligning the features between the source and target domains. For instance, Ganin et al. (2016) proposed Domain-Adversarial Neural Network (DANN) based on Generative Adversarial Networks (GAN) (Goodfellow et al., 2020). Long et al. (2018) transformed the adversarial conditions into domain discrimination information based on the correlation between classes and expanded the conditional adversarial mechanism. Tang and Jia (2020) proposed an integrated classifier for both class and domain classification to align the joint feature distributions across domains. Bousmalis et al. (2016) categorized feature representations into shared and private domains, modeling the uniqueness of each domain to enhance the ability to extract domain-invariant features. The above-mentioned methods aim to minimize the differences in feature distributions between the source and target domains to achieve domain alignment and subsequently employ source domain classifiers for discriminating target domain data.

Multi-Source Domain Adaptation (MSDA) allows for different distributions in the source domains and addresses the target domain discrimination problem by combining multiple source domains. However, the core idea of MSDA still involves aligning the various domain data through a shared network backbone (Peng et al., 2019; Guo et al., 2020; Zhao et al., 2018; Xu et al., 2018; Zhu et al., 2019; Rakshit et al., 2019). Some methods align domain distributions through weighting schemes. For example, Mansour et al. (2008) proposed distribution-weighted combination rules, where the target domain distribution is obtained as a weighted combination of multiple source domain distributions. By leveraging the relationships between the source domains and the target domain, using multiple source classifiers can yield optimal predictions for the target domain. Guo et al. (2018) explicitly learned the matching degree between source and target domain samples using meta-training based on point-to-set metric criteria to update the weight parameters for different source domains in relation to the target domain. Zhao et al. (2020) employed non-shared feature extractors to preserve more domain-discriminative features and achieved recognition on the target domain through weighted combinations of source classifiers. Other methods, such as M³SDA proposed by Peng et al. (2019), align the source domains with each other while aligning them with the target domain. Additionally, they collected and annotated a new domain adaptation dataset called DomainNet. Yang et al. (2020) utilized curriculum learning and adversarial learning to select the most suitable source domain samples for alignment with the target domain distribution. Wang et al. (2020) constructed a knowledge graph based on the prototypes of each source domain to aggregate existing knowledge from multiple domains, guiding the prediction of target domain samples. Nguyen et al. (2021) employed a joint feature extractor and combined multiple teachers in a mixture of source domains for global predictions.

Active Domain Adaptation (ADA) incorporates the idea of Active Learning (AL) (Fu et al., 2013; Geman et al., 1992; Huang et al., 2010; Ning et al., 2021), which aims to enhance model performance by actively selecting the most informative data for annotation, minimizing the annotation cost. Existing AL methods mostly rely on sample uncertainty (Wang et al., 2016; Tong and Koller, 2001; Vijayanarasimhan and Grauman, 2014) and representativeness (Gal et al., 2017) to assess the annotation value of samples. ADA methods draw inspiration from AL and aim to improve domain adaptation with limited annotations. Most ADA methods design query functions to rank the annotation value of target domain samples. For example, Su et al. (2020) applying AL to domain adaptation, represents targets based on the scores of domain discriminators and constructs a sample query function. Fu et al. (2021) proposed a random selection strategy to enhance sample diversity in the sample selection process. Another category of methods models the annotation value of target domain data based on clustering ideas. For instance, Prabhu et al. (2021) selects samples using uncertainty-weighted clustering within a clustering framework. These methods have achieved good results, but there are still limitations in considering certain aspects. For example, they do not take into account the domain similarity between different source domains and the target domain, as well as the inter-class similarity between different source domain classes and the target domain classes, which can lead to sample redundancy. It is worth noting that, unlike most AL and ADA methods, in our approach, the annotation of target domain data is achieved through pseudo-labeling rather than using their true labels. Fundamentally, it remains an unsupervised domain adaptation method.

3. Methodology

3.1. Problem definition

In our approach, we consider M labeled source domain datasets $S = \{S_1, S_1, S_1, \dots, S_M\}$ and one unlabeled target domain dataset T . Each source domain S_M contains N_{S_M} samples and label pairs $\{(x_i^{S_M}, y_i^{S_M})\}_{i=1}^{N_{S_M}}$, while the target domain data T only consists of N_T samples $X_T = \{x_i^T\}_{i=1}^{N_T}$, with unknown labels. However, the class space is shared among the source domains and the target domain, i.e., $C_{S_1} = C_{S_2} = \dots = C_{S_M} = C_{S_T}$, where C represents the class index ranging from 1 to K , and K is the number of classes.

In the multi-source active sampling process, we first initialize the labeled target domain sample set $T_L = \emptyset$. After training the model for a specified number of epochs, the model performs active sampling based on a sampling rate Δ . Then, we assign pseudo-labels y'_i to the selected target domain samples x'_i , forming labeled target domain data (x'_i, y'_i) that is added to T_L , and remove this data from the target domain T , denoted as $T = X_T / x'_i$. Finally, we train the model using the combined dataset $S \cup T_L$ and repeat the active sampling process in the next specified epoch.

Our objective is to fully consider the distinct distribution differences among multiple source domains and the target domain within the domain adaptation learning process. To achieve

this, we propose a dynamic weight adjustment mechanism that adapts to these differences. Furthermore, we employ active learning techniques to mitigate negative transfer during the domain adaptation process, while minimizing the cost of annotation.

3.2. Method framework

In this paper, we first define a weighted domain discrepancy loss function based on the distribution differences between each source domain and the target domain. We incorporate a dynamic weight adjustment mechanism during the learning process to control the adaptive learning weights of each source domain. Furthermore, we enhance the influence of challenging samples from the source domains on the decision boundary through a dynamic boundary loss, resulting in a clearer decision boundary. Based on this, we design a target domain sample query function for the active sampling strategy to assess the importance of unlabeled target samples. The proposed approach consists of two components: the dynamic domain discrepancy adjustment algorithm and the multi-source active boundary sample selection strategy.

Dynamic domain discrepancy adjustment algorithm consists of loss functions for each domain and their corresponding dynamic weight adjustment modules. Based on the overall distribution distances between the source domains and the target domain, the weights of the domain losses are dynamically adjusted for local samples in each training iteration. This adjustment aims to reduce loss oscillation and allow the target domain data to align more closely with the source domain samples that have higher relevance, promoting positive transfer and further enhancing model generalization.

we employ ResNet as the shared feature extractor. To mitigate the loss of metric features caused by the classification loss function and integrate the information extracted from different feature layers, we introduce a non-linear projection head $g(\cdot)$ after the shared feature extractor. This enhances the quality of representations extracted by the preceding layers of the network, thereby avoiding the issue of feature omission when measuring the domain discrepancy in subsequent steps. The non-linear projection head in our approach consists of two fully connected layers, as shown in Equation (1), where σ denotes the ReLU activation function. The dimensionality of the non-linear projection head is consistent with the output dimensionality of the shared feature extractor.

$$z = g(F(\cdot)) = W^{(2)}\sigma(W^{(1)}F) \quad (1)$$

The Domain-Level Alignment component employs the Maximum Mean Discrepancy (MMD) to assess the domain differences. Equation (2) represents the MMD in the Reproducing Kernel Hilbert Space (RKHS), where \mathcal{H} denotes the space associated with the kernel function. F represents the mapping function that maps the original features to the RKHS.

$$D_{\mathcal{H}}(F, p, q) \triangleq \sup_{f \in F} (\mathbb{E}_{x \sim p}[f(x)] - \mathbb{E}_{y \sim q}[f(y)]) \quad (2)$$

The domain discrepancy is quantified using Equation (3). $\widehat{D}_{\mathcal{H}}^{S_i}(p_{S_i}, p_T)$ represents the unbiased estimation of $D_{\mathcal{H}}^{S_i}(p_{S_i}, p_T)$,

where p_{S_i} and p_T denote the feature distributions of the source domain and target domain, respectively. The kernel function $\phi(\cdot)$ employed in the calculation utilizes a Gaussian kernel. By calculating the MMD distances between the feature distributions of each source and target domain, and incorporating them into the loss function, the distributions of the source and target domains are progressively aligned through iterative optimization. The domain discrepancy loss is expressed as Equation (4).

$$\widehat{D}_{\mathcal{H}}^{S_i}(X_{S_i}, X_T) \triangleq \left\| \frac{1}{N_{S_M}} \sum_{x^{S_i} \in X_{S_i}} [\phi(x^{S_i})] - \frac{1}{N_T} \sum_{x^T \in X_T} [\phi(x^T)] \right\|_{\mathcal{H}}^2 \quad (3)$$

$$\mathcal{L}_{mmd}^{S_i} = \widehat{D}_{\mathcal{H}}^{S_i}(z(X_{S_i}), z(X_T)) \quad (4)$$

Network maps the data from multiple source domains and the target domain to a shared feature space using the shared feature extractor F . During the training process, the network aims to minimize the distance between the feature distributions of the source domains and the target domain, as indicated by Equation (4). The cross-entropy loss function $\mathcal{L}_{clf}^{S_i}(F, C)$, defined in Equation (5), is used as the classification loss to optimize both the classifier C and the feature extractor F , N_{S_i} represents the size of the sample set in the source domain S_i , $y_j^{S_i}$ denotes the true label of the j -th sample $x_j^{S_i}$ in the source domain S_i , and $\widehat{y}_j^{S_i} \in (0, 1)$ represents the corresponding softMax prediction result.

$$\mathcal{L}_{clf}^{S_i}(F, C) = -\mathbb{E}_{(X_{S_i}, Y_{S_i}) \sim p_{S_i}} \frac{1}{N_{S_i}} \sum_{j=1}^{N_{S_i}} \sum_{k=1}^K y_j^{S_i} \log \widehat{y}_j^{S_i}(k) \quad (5)$$

Dynamic Weight Adjustment. In the process of domain adaptation, it is crucial to consider the distribution distances between source domains and the target domain in order to determine the weight parameters guiding the learning of the target domain. However, assigning equal weights to all samples within the same source domain and minimizing the domain discrepancy across all domains may result in negative transfer when certain source domain samples significantly differ from the target domain. To mitigate this issue, we propose a dynamic weight adjustment that adaptively adjusts the weights of source domains based on their distribution distances from the target domain. Through iterative modifications of the specific influence of each source domain, our algorithm dynamically selects source domain samples that are most relevant to the target domain samples, aiming to reduce the domain discrepancy between source and target domains and improve the accuracy of target domain sample classification.

Based on the pre-trained feature extraction network, we compute the overall distribution distances $\{D_{S_1}, D_{S_2}, \dots, D_{S_M}\}$ from each source domain $\{S_1, S_2, \dots, S_M\}$ to the target domain, as described in Equation (3). Assuming that the distribution distance between the source domain k and the target domain is the smallest, we apply an inverse transformation to the overall

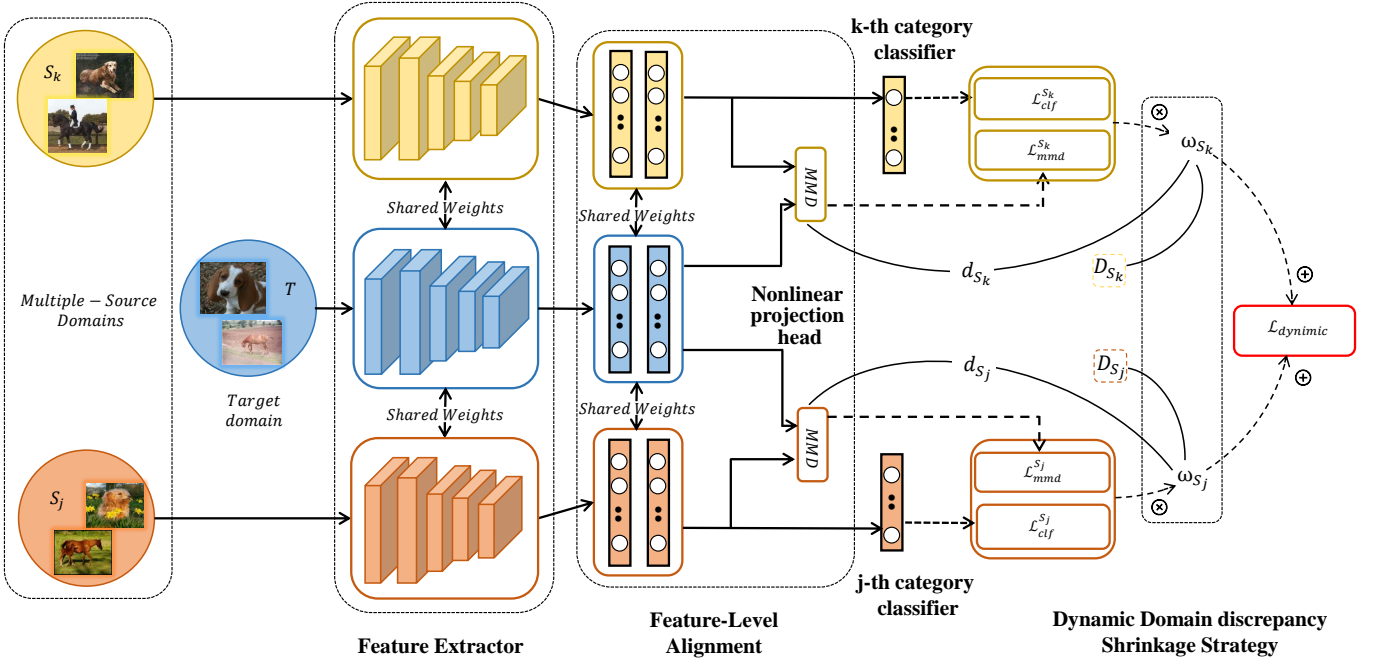


Figure 2: Overall framework of Dynamic Domain Discrepancy Adjustment algorithm. It contains four parts: shared feature extraction, nonlinear projection head, domain alignment, and multi-source classifier.

distribution distances and the distance between source domain k and the target domain $\{\frac{D_{S_k}}{D_{S_1}}, \frac{D_{S_k}}{D_{S_2}}, \dots, 1, \dots, \frac{D_{S_k}}{D_{S_M}}\}$, resulting in $\{\alpha_{S_1}, \alpha_{S_1}, \dots, \alpha_{S_k}, \dots, \alpha_{S_M}\}$. In each mini-batch, We first compute the batch-wise distribution distances $\{d_{S_1}, d_{S_2}, \dots, d_{S_M}\}$, by minimizing the domain discrepancy loss, we aim to narrow the distribution gaps between each source domain and the target domain. Based on the overall distances, we calculate the dynamic adjustment factor ω_{S_i} for source domain i using Equation (6), where ϵ_i is computed as $\frac{e^{-d_{S_i}}}{\sum_{j=1}^M e^{-d_{S_j}}}$. The sign of ϵ_i is determined by comparing the magnitudes of $\frac{D_{S_i}}{\sum_{j=1}^M D_{S_j}}$ and $\frac{d_{S_i}}{\sum_{j=1}^M d_{S_j}}$.

If $\frac{D_{S_i}}{\sum_{j=1}^M D_{S_j}} > \frac{d_{S_i}}{\sum_{j=1}^M d_{S_j}}$, ϵ_i is positive; otherwise, negative. During the domain adaptation training, the batch-wise distribution distances are used to adjust the impact strength of the overall distribution distances.

$$\omega_{S_i} = \alpha_{S_i} \pm \epsilon_{S_i} \quad (6)$$

Taking the source domains S_k and S_j as an example, the dynamic weight adjustment mechanism determines the dynamic adjustment factors ω_{S_k} and ω_{S_j} for source domains k and j , respectively, based on the overall distribution distances D_{S_k} and D_{S_j} between the source domains and the target domain. These factors are computed using the batch-wise adjusted distances d_{S_k} and d_{S_j} during the iterative process. By incorporating the dynamic adjustment factors, the network can leverage more relevant source domain sample features in each training iteration, allowing the target domain to benefit from the information provided by the source domains that are more closely related to it. This dynamic adjustment enables the target domain to effectively utilize the features of the related source domain samples

during every training process.

The dynamic domain discrepancy loss function is defined as equation (7), where β is a hyperparameter that controls the weight of domain adaptation and its optimal value for the single-source domain scenario is determined empirically. $\mathcal{L}_{clf}^{S_i}(\cdot)$ represents the classification loss for the i -th source domain, and $\mathcal{L}_{mmd}^{S_i}(\cdot)$ represents the domain discrepancy loss for that source domain. ω_{S_i} is the dynamic adjustment factor for the source domain S_i .

$$\mathcal{L}_{dynamic} = \sum_{i=1}^M \omega_{S_i} (\mathcal{L}_{clf}^{S_i}(F, C) + \beta \mathcal{L}_{mmd}^{S_i}) \quad (7)$$

Multi-source Active Boundary Sample Selection strategy.

To alleviate the source domain bias, we introduce a simple dynamic boundary loss term, as shown in Equation (8). The term $[C(z(x))_i - C(z(x))_y + d]_+$ ensures that the larger value between 0 and $[C(z(x))_i - C(z(x))_y + d]$ is taken, where d is a hyperparameter that determines the desired boundary. Here, $C(\cdot)_i$ and $C(\cdot)_y$ represent the outputs of the classifier for the i -th class and the true class, respectively. By incorporating Equation (8) into the training process, the model focuses more on difficult samples that are challenging to discriminate in each source domain, thus enhancing the model's classification capability. This dynamic boundary loss term encourages the model to pay greater attention to samples near the decision boundaries, which leads to an improved decision boundary and overall classification performance.

$$\mathcal{L}_{dis}(x^{S_i}, y^{S_i}) = \sum_{k=1}^K \omega_{S_i} [C(z(x^{S_i}))_k - C(z(x^{S_i}))_y + d]_+ \quad (8)$$

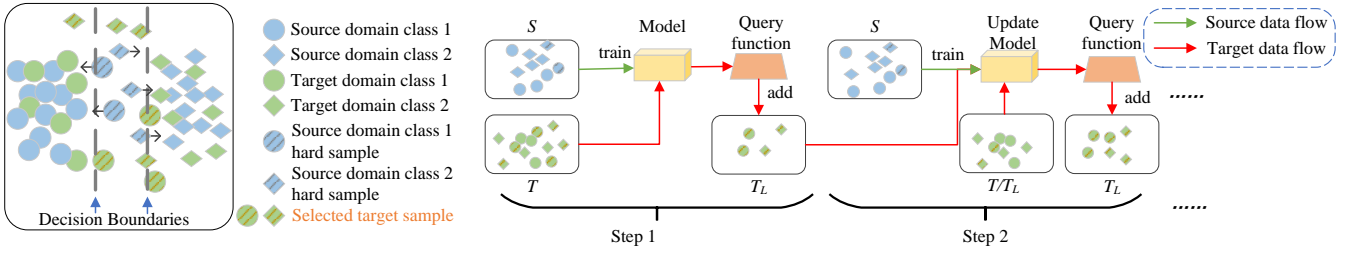


Figure 3: Active sample screening strategy. Firstly, the hard samples of each category are kept away from the classification boundary by dynamic boundary loss, which in turn expands the decision boundary between categories, and secondly, the samples in the target domain data that are at the decision boundary are screened and labeled by our query function to expand the labeled target domain sample set T_L .

The dynamic boundary loss allows us to determine that for the target domain data, the smaller the discrepancy in the classification outputs among different classes obtained by the soft-Max layer, the greater the influence of that data on the decision boundary. Based on this characteristic, we design a query function, as shown in Equation (9), to obtain the ranking of sample importance in the target domain.

In the query function, when a sample exhibits more balanced predictions among different classes, indicating higher uncertainty in the model’s predictions, the sample is assigned a higher importance score. The term $\text{softMax}(C(z(x^T)))_i$ represents the i -th value in the logit vector obtained by sorting the output of the softmax layer in descending order.

$$I(x^T) = 1 - [\text{softMax}(C(z(x^T)))_1 - \text{softMax}(C(z(x^T)))_2] \quad (9)$$

We can sort the samples from the target domain based on their importance scores obtained from Equation (9). Then, we select the top-ranked samples according to a given sampling rate, assign pseudo-labels to these samples, and include them in the labeled target domain sample set, T_L . Finally, we update the model using the combined dataset, $T_L \cup S$, where S represents the labeled source domain samples.

4. Experiments

To verify the effectiveness of our method, we draw on the dataset used in the literature related to active domain adaption (Su et al., 2020; Fu et al., 2021; Prabhu et al., 2021) to validate the performance of our method and further analyze the experimental results.

4.1. Data description

we conducted performance testing of our method using the Office-31, Office-Caltech 10, and Office-Home datasets. The Office-31 dataset (Saenko et al., 2010) consists of 4,652 images collected from office environments. It includes three domains: Amazon (A), DSLR (D), and Webcam (W). Each domain contains the same 31 categories. In our experiments, we selected one domain as the target domain and used the other two domains as the source domains, creating three transfer tasks. The Office-Caltech 10 dataset (Chen et al., 2020) is derived from

the Office-31 dataset and the Caltech-256 dataset. It contains a total of 2,533 images from four domains: Amazon (A), DSLR (D), Webcam (W), and Caltech (C). The dataset consists of 10 common categories across domains. We selected three subsets from the Office-Caltech 10 dataset as the source domains and used the remaining subset as the target domain, creating four transfer tasks. The Office-Home dataset (Venkateswara et al., 2017) consists of four domains: Art (A), Clipart (C), Product (P), and Real-World (R). It contains a total of 65 categories, and the category labels are consistent across domains. We selected three subsets from the Office-Home dataset as the source domains and used the remaining subset as the target domain, creating four transfer tasks.

4.2. Experiment setup

We conducted several comparative experiments in this section using different datasets. Firstly, we compared our approach with a baseline where only the source domain data is used for training. Secondly, we compared our method with several classical single-source domain adaptation methods, including Transfer Component Analysis (TCA) (Pan et al., 2011), Geodesic Flow Kernel (GFK) (Gong et al., 2012), Deep Domain Confusion (DDC) (Tzeng et al., 2014), Deep CORAL (Sun and Saenko, 2016), Reversed Gradient (RevGrad) (Ganin and Lempitsky, 2015), Domain Adaptation Network (DAN) (Long et al., 2015), Residual Transfer Network (RTN) (Long et al., 2016), Joint Adaptation Network (JAN) (Long et al., 2017), Manifold Embedded Distribution Alignment (MEDA) (Wang et al., 2018), Maximum Classifier Discrepancy (MCD) (Saito et al., 2018), Adversarial Discriminative Domain Adaptation (ADDA) (Tzeng et al., 2017), CDT (Xu et al., 2021), FixBi (Na et al., 2021), and single-source active domain adaptation methods such as UCN (Joshi et al., 2012), QBC (Dagan and Engelson, 1995), Clustering (Nguyen and Smeulders, 2004), AADA (Su et al., 2020), ADMA (Huang et al., 2018), TQS (Fu et al., 2021), and CLUE (Prabhu et al., 2021).

For the single-source domain adaptation experiments, we employed two strategies. The first strategy is the Single-Best method, where each source domain is independently adapted to the target domain, and the highest recognition accuracy among the source domains is chosen as the final result. The second strategy is the Source-Combine method, where all the source domain data is combined into a single dataset, and a

single-source domain adaptation method is applied to solve the multi-source adaptation problem. This strategy aims to explore whether incorporating data from other source domains can improve the performance of single-source domain adaptation.

Finally, we compared our method with several state-of-the-art multi-source deep domain adaptation methods, including Deep Cocktail Network (DCTN) (Xu et al., 2018), Multi-Source Distilling Domain Adaptation (MDDA) (Zhao et al., 2020), Multi-Source Domain Adversarial Networks (MDAN) (Zhao et al., 2018), Moment Matching for Multi-Source DA (M³SDA) (Peng et al., 2019), Learning to Combine for Multi-Source Domain Adaptation (Ltc-MSDA) (Wang et al., 2020), SImpAI (Venkat et al., 2020), DARN (Wen et al., 2020), SHOT (Liang et al., 2021), MFSAN (Zhu et al., 2019), STEM (Nguyen et al., 2021), DINE (Liang et al., 2022), PTMDA (Ren et al., 2022), and Curriculum Manager for Source Selection (CMSS) (Yang et al., 2020).

Method	Model	A, D→W	A, W→D	D, W→A	Avg
Single-best	Source Only	96.7	99.3	62.5	86.2
	TCA	96.7	99.6	63.7	86.7
	GFK	95.0	98.2	65.4	86.2
	DDC	95.2	98.2	67.4	86.9
	CORAL	98.0	99.7	65.3	87.7
	RevGrad	96.9	99.2	68.2	88.1
	DAN	96.8	99.6	66.8	87.7
	RTN	96.8	99.6	66.2	87.5
	FixBi	99.3	100.0	79.4	92.9
	CDT	99.0	100.0	76.5	91.8
Source-combine	RevGrad	98.1	99.7	67.6	88.5
	CORAL	98.0	99.3	67.1	88.1
	DAN	97.8	99.6	67.6	88.3
Multi-source	DCTN	96.9	99.6	54.9	83.8
	MDAN	95.4	99.2	55.2	83.3
	MDDA	97.1	99.2	56.2	84.2
	Ltc-MSDA	97.2	99.6	56.9	84.6
	DINE	98.4	100.0	76.8	91.5
	PTMDA	99.6	100.0	75.4	91.7
	Ours	100.0	100.0	81.3	93.8

Table 1: Classification accuracy (%) on the Office-31 dataset

Our method is implemented based on PyTorch. We fine-tune all the layers of the pre-trained ResNet-50 model trained on ImageNet using the source domain data. We also train the non-linear projection head and the classifier. We utilize the stochastic gradient descent (SGD) optimizer with a momentum of 0.9. The learning rate is set to ten times the learning rate of the feature extractor.

In addition, we apply exponential decay to the learning rate during training iterations, as shown in Equation (10), where lr_{init} represents the initial learning rate, which is set to 0.01, $\gamma = 0.8$, epoch denotes the current number of training epochs, and $epoch_{drop}$ is set to 10. Our sampling strategy takes effect from the 20th epoch onwards, with sampling performed every 2 epochs. The sampling rate is set to $\Delta = 0.01$, and we conduct 5 rounds of sampling.

$$lr_{new} = lr_{init} \times \gamma^{(1+epoch)/epoch_{drop}} \quad (10)$$

4.3. Experiment results and analysis

The experimental results of our method on the Office-31, Office-Home, and Office-Caltech 10 datasets are shown in Tables 1, 2, and 3, respectively. In the tables, "source-only" indicates applying the model trained solely on the source domain directly to the target domain for testing. "single-best" refers to using single-source domain adaptation methods to transfer each source domain to the target domain and selecting the highest accuracy as the reported result. Furthermore, we compared our method with several advanced single-source active domain adaptation methods on the Office-31 dataset. Since our method is designed for multi-source settings, we report the average classification accuracy of the single-source methods across all source domains to the same target domain as the model's accuracy on that target domain. The experimental results are presented in Table 4.

As shown in Table 1, our method achieves state-of-the-art recognition accuracy on the Office-31 dataset. Particularly, in the challenging task where the target domain is Amazon, our method outperforms the current state-of-the-art method by 4.5% in terms of recognition accuracy. The overall average accuracy of our method across the three transfer tasks surpasses the second-best method by 2.5%.

Method	Model	C,PR→A	A,PR→C	A,C,R→P	A,C,P→R	Avg
Single Best	Source only	65.3	49.6	79.7	75.4	67.5
	DDC	64.1	50.8	78.2	75.0	67
	DAN	68.2	56.5	80.3	75.9	70.2
	RevGrad	67.9	55.9	80.4	75.8	70
Source Combine	DAN	68.5	59.4	79.0	82.5	72.4
	Deep CORAL	68.1	58.6	79.5	82.7	72.2
	RevGrad	68.4	59.1	79.5	82.7	72.4
Multi-Source	SImpAI50	70.8	56.3	80.2	81.5	72.2
	SImpAI100	73.4	62.4	81.0	82.7	74.8
	DARN	70.0	68.4	82.7	83.9	76.3
	SHOT++	73.1	61.3	84.3	84.0	75.7
	MDDA	66.7	62.3	79.5	79.6	71
	MFSAN	72.1	62.0	80.3	81.8	74.1
	Ours	75.4	62.3	85.1	84.4	76.8

Table 2: Classification accuracy (%) on Office-Home dataset.

In Table 2, We can see our model demonstrates superior performance in the To→W, To→D, and To→C tasks. The overall average accuracy of our method exhibits a 1.4% improvement compared to the current state-of-the-art method.

Table 3 reveals that our method achieves the highest recognition accuracy in the To→W, To→D, and To→C transfer tasks of the Office-Caltech 10 dataset. In the To→A task, our method falls only 0.1% short of the best-performing method. Across all four transfer tasks, our method consistently achieves the highest average recognition accuracy.

Referring to the data in Table 4, under the constraint of the same annotation budget, our method achieves 100% accuracy in the To→D and To→D tasks. Moreover, our method surpasses the second-best single-source method by 1.74% in terms of overall average accuracy, thereby validating the efficacy of our proposed sampling strategy.

In addition, we visualized the clustering of latent features of the source and target domains before and after domain adaptation using T-SNE in our method. Figure 4 demonstrates that

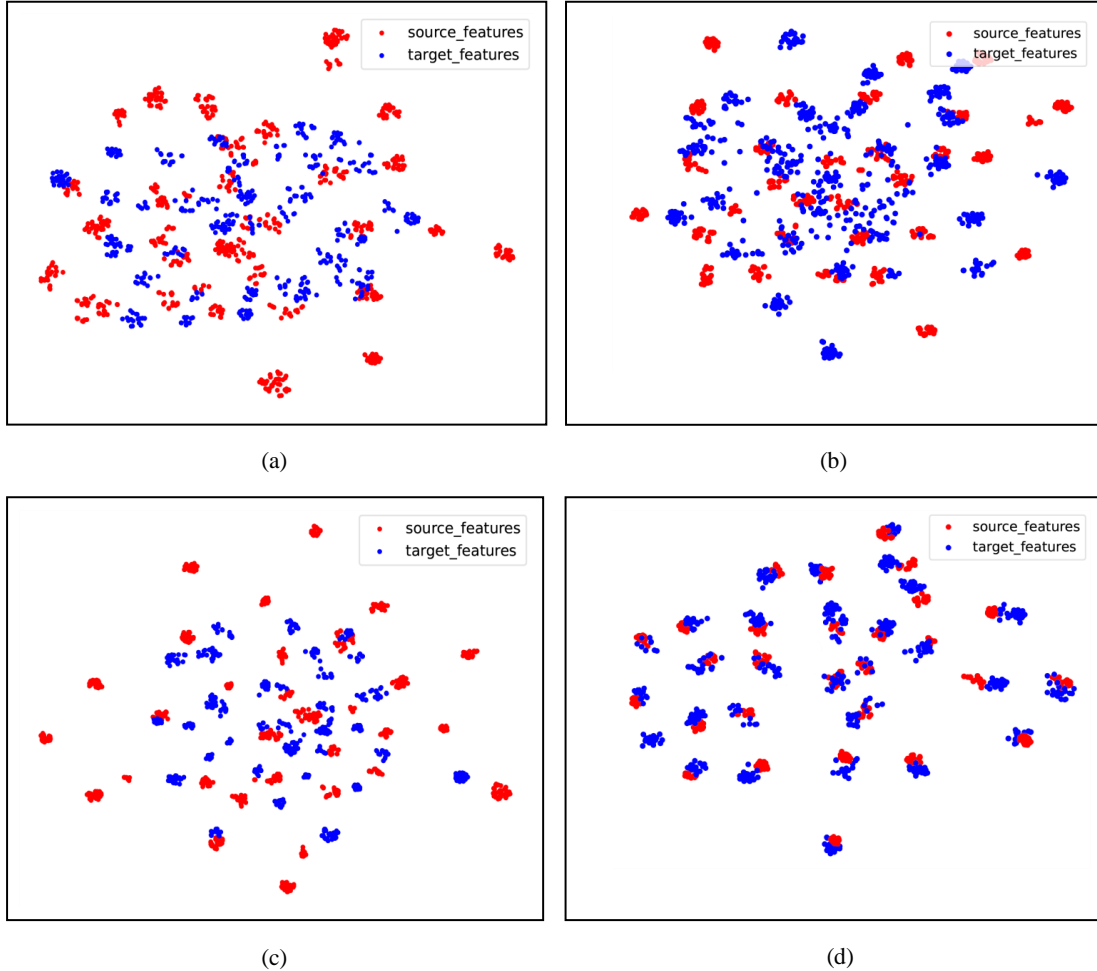


Figure 4: T-SNE: Results of feature distribution visualization on the Office-31 dataset. (a), (b), (c) and (d) indicate the results of training with source domain only, adding dynamic domain difference adjustment, adding dynamic boundary loss, and the overall D^3 AAMDA method, respectively. (d) demonstrates that the method in this paper can effectively align the source and target domain feature distributions.

Method	Model	A, C, D→W	A, C, W→D	A, D, W→C	C, D, W→A	Avg
Source Only	Source Only	99.0	98.3	87.8	86.1	92.8
	DAN	99.3	98.2	89.7	94.8	95.5
Source Combine	Source only	99.1	98.2	85.4	88.7	92.9
	DAN	99.5	99.1	89.2	91.6	94.8
	DCTN	99.4	99.0	90.2	92.7	95.3
	JAN	99.4	99.4	91.2	91.8	95.5
	MEDA	99.3	99.2	91.4	92.9	95.7
	MCD	99.5	99.1	91.5	92.1	95.6
Multi-Source	M ³ SDA	99.5	99.2	92.2	94.5	96.4
	CMSS	99.6	99.3	93.7	96.6	97.2
	STEM	100.0	100.0	94.2	98.4	98.2
	Ours	100.0	100.0	96.5	98.3	98.7

Table 3: Classification accuracy (%) on the Office- Caltech 10 dataset.

each module of our method has a positive effect on aligning the features of the source and target domains.

4.4. Ablation analysis

To further investigate the effectiveness of the proposed improvements, we conducted ablation experiments. The ablation comparison modules mainly include the parameters α and ϵ that constitute the dynamic domain discrepancy adjustment factor ω (α is calculated based on the overall distribution distance between each source domain and the target domain, de-

Method	To→A	To→D	To→W	Avg
ResNet	64.40	90.45	85.10	79.98
RAN	75.65	93.35	91.10	86.70
UCN	78.40	94.90	93.45(D→W:100)	88.92
QBC	77.60	94.65	92.95	88.40
Cluster	76.80	93.85	92.15	87.60
AADA	78.45	94.60	93.40(D→W:100)	88.82
ADMA	79.15	95.00(W→D:100)	94.15(D→W:100)	89.43
CLUE	76.10	95.70(W→D:100)	93.35	88.38
SDM	81.90	97.40(W→D:100)	96.75(D→W:100)	92.02
TQS	80.50	96.40(W→D:100)	96.10(D→W:100)	91.00
Ours	81.33	100.00	100.00	93.76

Table 4: Classification accuracy (%) on the Office-31 dataset with the budget of 5% data. Since existing active domain adaptation methods are designed for single-source settings, we compare our multi-source settings by taking the average classification accuracy of each domain in the single-source method and treating it as the classification accuracy of the model for the target domain. “RAN” represents random sampling. “(D→W:100)” indicates a classification accuracy of 100 achieved under the D→W setting.”

α	ϵ	Nonlinear Projection Head	Dynamic boundary loss	Active boundary sampling	Office-31			
					A, D→W	A, W→D	D, W→A	Avg
✓	×	×	×	×	97.6	99.4	67.1	88.0
×	✓	✓	×	×	98.5	99.4	67.5	88.5
✓	×	✓	×	×	98.9	99.6	69.7	89.4
✓	✓	×	×	×	98.7	100.0	68.8	89.2
✓	✓	✓	×	×	99.0	100.0	71.6	90.2
✓	✓	✓	✓	×	99.2	100.0	72.4	90.5
✓	✓	✓	×	✓	99.6	100.0	75.6	91.7
✓	✓	✓	✓	✓	100.0	100.0	81.3	93.8

Table 5: Ablation Experiments Result. We analyze these important components by using or removing them on the ResNet-50 backbone and Office-31 datasets.

terminating the proportion of each source domain in the overall loss function, and ϵ serves as a correction term to further adjust α based on the distribution distance obtained during batch training), the non-linear projection head, the dynamic boundary loss, and the proposed active boundary sample selecting strategy. The ablation experiments led to the following conclusions: (1) The α determined by transforming the overall distribution distance between each source domain and the target domain can select source domains that are more similar to the target domain, which plays a major role in balancing the loss functions of different source domains. (2) The ϵ determined by transforming the batch distribution distance between each source domain and the target domain can also select source domains with higher similarity to the target domain to some extent, but it may lead to training instability and noticeable oscillations during the training process. (3) The dynamic boundary loss can further increase the distance between decision boundaries of different classes, thereby improving classification accuracy.

Furthermore, to verify the effectiveness of our active boundary sample selecting strategy, we compared it with random sampling and cluster center sampling on the Office-31 dataset. The sampling rate was set to $\Delta = 0.01$, and each experiment was performed five times. The experimental results are shown in Table 6.

sampling strategy	A, D→W	A, W→D	D, W→A	Avg
random sampling	99.4	100.0	76.4	91.9
Cluster center sampling	99.5	100.0	78.6	92.7
Active boundary sampling	100.0	100.0	81.3	93.8

Table 6: Impact of different sampling strategies.

The experimental results demonstrate that our active boundary sample selecting strategy can effectively select important samples that are most beneficial for target domain classification. It outperforms other sampling strategies in terms of efficiency in improving the recognition rate of the target domain. This further validates the effectiveness of our overall method in addressing the problem of multi-source unsupervised domain adaptation.

5. Discussion

In this paper, we propose a novel approach called Dynamic Domain Discrepancy Adjustment for Active Multi-Domain Adaptation (D^3 AAMDA) that applies active learning to the problem of multi-source domain adaptation. D^3 AAMDA consists of two main components. Firstly, we introduce the Dynamic Domain Discrepancy Adjustment algorithm, which dynamically adjusts the influence of each source domain on the target domain during the domain adaptation process. This allows the target domain to leverage more relevant source domain sample features. Secondly, we propose a Dynamic Boundary Loss that focuses on the contribution of difficult samples around the decision boundaries, thereby enlarging the inter-class decision boundary distances. Additionally, we incorporate an Active Boundary Sample Selecting strategy to extract important samples from the target domain, thereby enhancing the model training with minimal annotation cost. We compare our approach with several advanced domain adaptation methods, and extensive experimental analyses demonstrate the superiority of our proposed approach. In the future, we aim to extend domain adaptation methods to address the challenges of multi-modal domains and improve the generalizability of the models.

References

- Bousmalis, K., Trigeorgis, G., Silberman, N., Krishnan, D., Erhan, D., 2016. Domain separation networks. *Advances in neural information processing systems* 29.
- Chen, X., Fan, H., Girshick, R., He, K., 2020. Improved baselines with momentum contrastive learning. *arXiv preprint arXiv:2003.04297*.
- Courty, N., Flamary, R., Habrard, A., Rakotomamonjy, A., 2017. Joint distribution optimal transportation for domain adaptation. *Advances in neural information processing systems* 30.
- Dagan, I., Engelson, S.P., 1995. Committee-based sampling for training probabilistic classifiers, in: *Machine Learning Proceedings 1995*. Elsevier, pp. 150–157.
- Damodaran, B.B., Kellenberger, B., Flamary, R., Tuia, D., Courty, N., 2018. Deepjdot: Deep joint distribution optimal transport for unsupervised domain adaptation, in: *Proceedings of the European conference on computer vision (ECCV)*, pp. 447–463.
- Fu, B., Cao, Z., Wang, J., Long, M., 2021. Transferable query selection for active domain adaptation, in: *Proceedings of the IEEE/CVF Conference on Computer Vision and Pattern Recognition*, pp. 7272–7281.
- Fu, Y., Zhu, X., Li, B., 2013. A survey on instance selection for active learning. *Knowledge and information systems* 35, 249–283.

- Gal, Y., Islam, R., Ghahramani, Z., 2017. Deep bayesian active learning with image data, in: International conference on machine learning, PMLR. pp. 1183–1192.
- Ganin, Y., Lempitsky, V., 2015. Unsupervised domain adaptation by back-propagation, in: International conference on machine learning, PMLR. pp. 1180–1189.
- Ganin, Y., Ustinova, E., Ajakan, H., Germain, P., Larochelle, H., Laviolette, F., Marchand, M., Lempitsky, V., 2016. Domain-adversarial training of neural networks. *The journal of machine learning research* 17, 2096–2030.
- Geman, S., Bienenstock, E., Doursat, R., 1992. Neural networks and the bias/variance dilemma. *Neural computation* 4, 1–58.
- Gong, B., Shi, Y., Sha, F., Grauman, K., 2012. Geodesic flow kernel for unsupervised domain adaptation, in: 2012 IEEE conference on computer vision and pattern recognition, IEEE. pp. 2066–2073.
- Goodfellow, I., Pouget-Abadie, J., Mirza, M., Xu, B., Warde-Farley, D., Ozair, S., Courville, A., Bengio, Y., 2020. Generative adversarial networks. *Communications of the ACM* 63, 139–144.
- Guo, H., Pasunuru, R., Bansal, M., 2020. Multi-source domain adaptation for text classification via distancenet-bandits, in: Proceedings of the AAAI conference on artificial intelligence, pp. 7830–7838.
- Guo, J., Shah, D.J., Barzilay, R., 2018. Multi-source domain adaptation with mixture of experts. arXiv preprint arXiv:1809.02256 .
- Huang, S.J., Jin, R., Zhou, Z.H., 2010. Active learning by querying informative and representative examples. *Advances in neural information processing systems* 23.
- Huang, S.J., Zhao, J.W., Liu, Z.Y., 2018. Cost-effective training of deep cnns with active model adaptation, in: Proceedings of the 24th ACM SIGKDD International Conference on Knowledge Discovery & Data Mining, pp. 1580–1588.
- Joshi, A.J., Porikli, F., Papanikolopoulos, N.P., 2012. Scalable active learning for multiclass image classification. *IEEE transactions on pattern analysis and machine intelligence* 34, 2259–2273.
- Kang, G., Jiang, L., Yang, Y., Hauptmann, A.G., 2019. Contrastive adaptation network for unsupervised domain adaptation, in: Proceedings of the IEEE/CVF conference on computer vision and pattern recognition, pp. 4893–4902.
- Liang, J., Hu, D., Feng, J., He, R., 2022. Dine: Domain adaptation from single and multiple black-box predictors, in: Proceedings of the IEEE/CVF Conference on Computer Vision and Pattern Recognition, pp. 8003–8013.
- Liang, J., Hu, D., Wang, Y., He, R., Feng, J., 2021. Source data-absent unsupervised domain adaptation through hypothesis transfer and labeling transfer. *IEEE Transactions on Pattern Analysis and Machine Intelligence* 44, 8602–8617.
- Long, M., Cao, Y., Wang, J., Jordan, M., 2015. Learning transferable features with deep adaptation networks, in: International conference on machine learning, PMLR. pp. 97–105.
- Long, M., Cao, Z., Wang, J., Jordan, M.I., 2018. Conditional adversarial domain adaptation. *Advances in neural information processing systems* 31.
- Long, M., Zhu, H., Wang, J., Jordan, M.I., 2016. Unsupervised domain adaptation with residual transfer networks. *Advances in neural information processing systems* 29.
- Long, M., Zhu, H., Wang, J., Jordan, M.I., 2017. Deep transfer learning with joint adaptation networks, in: International conference on machine learning, PMLR. pp. 2208–2217.
- Mansour, Y., Mohri, M., Rostamizadeh, A., 2008. Domain adaptation with multiple sources. *Advances in neural information processing systems* 21.
- Na, J., Jung, H., Chang, H.J., Hwang, W., 2021. Fixbi: Bridging domain spaces for unsupervised domain adaptation, in: Proceedings of the IEEE/CVF conference on computer vision and pattern recognition, pp. 1094–1103.
- Nguyen, H.T., Smeulders, A., 2004. Active learning using pre-clustering, in: Proceedings of the twenty-first international conference on Machine learning, p. 79.
- Nguyen, V.A., Nguyen, T., Le, T., Tran, Q.H., Phung, D., 2021. Stem: An approach to multi-source domain adaptation with guarantees, in: Proceedings of the IEEE/CVF International Conference on Computer Vision, pp. 9352–9363.
- Ning, K.P., Tao, L., Chen, S., Huang, S.J., 2021. Improving model robustness by adaptively correcting perturbation levels with active queries, in: Proceedings of the AAAI Conference on Artificial Intelligence, pp. 9161–9169.
- Pan, S.J., Tsang, I.W., Kwok, J.T., Yang, Q., 2011. Domain adaptation via transfer component analysis. *IEEE Transactions on Neural Networks* 22, 199–210. doi:10.1109/TNN.2010.2091281.
- Peng, X., Bai, Q., Xia, X., Huang, Z., Saenko, K., Wang, B., 2019. Moment matching for multi-source domain adaptation, in: Proceedings of the IEEE/CVF international conference on computer vision, pp. 1406–1415.
- Prabhu, V., Chandrasekaran, A., Saenko, K., Hoffman, J., 2021. Active domain adaptation via clustering uncertainty-weighted embeddings, in: Proceedings of the IEEE/CVF International Conference on Computer Vision, pp. 8505–8514.
- Rakshit, S., Banerjee, B., Roig, G., Chaudhuri, S., 2019. Unsupervised multi-source domain adaptation driven by deep adversarial ensemble learning, in: Pattern Recognition: 41st DAGM German Conference, DAGM GCPR 2019, Dortmund, Germany, September 10–13, 2019, Proceedings 41, Springer. pp. 485–498.
- Ren, C.X., Liu, Y.H., Zhang, X.W., Huang, K.K., 2022. Multi-source unsupervised domain adaptation via pseudo target domain. *IEEE Transactions on Image Processing* 31, 2122–2135.
- Saenko, K., Kulis, B., Fritz, M., Darrell, T., 2010. Adapting visual category models to new domains, in: Computer Vision–ECCV 2010: 11th European Conference on Computer Vision, Heraklion, Crete, Greece, September 5–11, 2010, Proceedings, Part IV 11, Springer. pp. 213–226.
- Saito, K., Watanabe, K., Ushiku, Y., Harada, T., 2018. Maximum classifier discrepancy for unsupervised domain adaptation, in: Proceedings of the IEEE conference on computer vision and pattern recognition, pp. 3723–3732.
- Su, J.C., Tsai, Y.H., Sohn, K., Liu, B., Maji, S., Chandraker, M., 2020. Active adversarial domain adaptation, in: Proceedings of the IEEE/CVF Winter Conference on Applications of Computer Vision, pp. 739–748.
- Sun, B., Saenko, K., 2016. Deep coral: Correlation alignment for deep domain adaptation, in: Computer Vision–ECCV 2016 Workshops: Amsterdam, The Netherlands, October 8–10 and 15–16, 2016, Proceedings, Part III 14, Springer. pp. 443–450.
- Tang, H., Jia, K., 2020. Discriminative adversarial domain adaptation, in: Proceedings of the AAAI conference on artificial intelligence, pp. 5940–5947.
- Tong, S., Koller, D., 2001. Support vector machine active learning with applications to text classification. *Journal of machine learning research* 2, 45–66.
- Tzeng, E., Hoffman, J., Saenko, K., Darrell, T., 2017. Adversarial discriminative domain adaptation, in: Proceedings of the IEEE conference on computer vision and pattern recognition, pp. 7167–7176.
- Tzeng, E., Hoffman, J., Zhang, N., Saenko, K., Darrell, T., 2014. Deep domain confusion: Maximizing for domain invariance. arXiv preprint arXiv:1412.3474 .
- Venkat, N., Kundu, J.N., Singh, D., Revanur, A., et al., 2020. Your classifier can secretly suffice multi-source domain adaptation. *Advances in Neural Information Processing Systems* 33, 4647–4659.
- Venkateswara, H., Eusebio, J., Chakraborty, S., Panchanathan, S., 2017. Deep hashing network for unsupervised domain adaptation, in: Proceedings of the IEEE conference on computer vision and pattern recognition, pp. 5018–5027.
- Vijayanarasimhan, S., Grauman, K., 2014. Large-scale live active learning: Training object detectors with crawled data and crowds. *International journal of computer vision* 108, 97–114.
- Wang, H., Xu, M., Ni, B., Zhang, W., 2020. Learning to combine: Knowledge aggregation for multi-source domain adaptation, in: Computer Vision–ECCV 2020: 16th European Conference, Glasgow, UK, August 23–28, 2020, Proceedings, Part VIII 16, Springer. pp. 727–744.
- Wang, J., Feng, W., Chen, Y., Yu, H., Huang, M., Yu, P.S., 2018. Visual domain adaptation with manifold embedded distribution alignment, in: Proceedings of the 26th ACM international conference on Multimedia, pp. 402–410.
- Wang, K., Zhang, D., Li, Y., Zhang, R., Lin, L., 2016. Cost-effective active learning for deep image classification. *IEEE Transactions on Circuits and Systems for Video Technology* 27, 2591–2600.
- Wen, J., Greiner, R., Schuurmans, D., 2020. Domain aggregation networks for multi-source domain adaptation, in: International conference on machine learning, PMLR. pp. 10214–10224.
- Xu, R., Chen, Z., Zuo, W., Yan, J., Lin, L., 2018. Deep cocktail network: Multi-source unsupervised domain adaptation with category shift, in: Proceedings of the IEEE conference on computer vision and pattern recognition, pp. 3964–3973.
- Xu, T., Chen, W., Wang, P., Wang, F., Li, H., Jin, R., 2021. Cdtrans: Cross-domain transformer for unsupervised domain adaptation. arXiv preprint arXiv:2109.06165 .
- Yang, L., Balaji, Y., Lim, S.N., Shrivastava, A., 2020. Curriculum manager for

source selection in multi-source domain adaptation, in: Computer Vision–ECCV 2020: 16th European Conference, Glasgow, UK, August 23–28, 2020, Proceedings, Part XIV 16, Springer. pp. 608–624.

Zhao, H., Zhang, S., Wu, G., Moura, J.M., Costeira, J.P., Gordon, G.J., 2018. Adversarial multiple source domain adaptation. *Advances in neural information processing systems* 31.

Zhao, S., Wang, G., Zhang, S., Gu, Y., Li, Y., Song, Z., Xu, P., Hu, R., Chai, H., Keutzer, K., 2020. Multi-source distilling domain adaptation, in: Proceedings of the AAAI Conference on Artificial Intelligence, pp. 12975–12983.

Zhu, Y., Zhuang, F., Wang, D., 2019. Aligning domain-specific distribution and classifier for cross-domain classification from multiple sources, in: Proceedings of the AAAI conference on artificial intelligence, pp. 5989–5996.